Food Chemistry 375 (2022) 131680

Contents lists available at ScienceDirect

Food Chemistry

journal homepage: www.elsevier.com/locate/foodchem

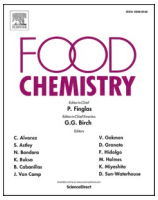

The key food odorant receptive range of broadly tuned receptor OR2W1

Franziska Haag, Antonella Di Pizio, Dietmar Krautwurst *

Leibniz-Institute for Food Systems Biology at the Technical University of Munich, Lise-Meitner-Str. 34, 85354 Freising, Germany

ARTICLE INFO

Keywords:
Olfaction
Chemosensory
GPCR
Agonist chemotypes
Potency

ABSTRACT

Mammals perceive a multitude of odorants by their chemical sense of olfaction, a high-dimensional stimulus-detection system, with hundreds of narrowly or broadly tuned receptors, enabling pattern recognition by the brain. Cognate receptor-agonist information, however, is sparse, and the role of broadly tuned odorant receptors for encoding odor quality remains elusive. Here, we screened IL-6-HaloTag®-OR2W1 and haplotypes against 187 out of 230 defined key food odorants using the GloSensor™ system in HEK-293 cells, yielding 48 new agonists. Altogether, key food odorants represent about two-thirds of now 153 reported agonists of OR2W1, the highest number of agonists known for a mammalian odorant receptor. In summary, we characterized OR2W1 as a human odorant receptor, with a chemically diverse but exclusive receptive range, complementary to chemical subgroups covered by evolutionary younger, highly selective receptors. Our data suggest OR2W1 to be suited for participating in the detection of many foodborne odorants.

1. Introduction

The chemosensory perception of a multitude of odors is initiated by the interaction of odorant molecules, preferably of ecological relevance, such as key food odorants (KFOs) or semiochemicals, with G protein-coupled receptors (GPCRs) in the nose (Barwich, 2016), encoded by ca. 400 odorant receptor (OR) genes in humans (Malnic, Godfrey, & Buck, 2004; Olender et al., 2012). ORs may be narrowly tuned (Haag, Hoffmann, & Krautwurst, 2021; NOE, Polster, Geithe, Kotthoff, Schieberle, & Krautwurst, 2017) or rather broadly tuned (Baud et al., 2011; Geithe, NOE, Kreissl, & Krautwurst, 2017; J. Li, Haddad, Chen, Santos, & Luetje, 2012; Tazir, Khan, Mombaerts, & Grosmaitre, 2016). An interaction of adequate stimuli at the receptor level, thus, often appears to be governed by a combinatorial code, such that individual receptors can recognize multiple odorants, and individual odorants may be detected by multiple ORs (Malnic, Hirono, Sato, & Buck, 1999; Nara, Saraiva, Ye, & Buck, 2011), inducing activity patterns in the olfactory central nervous system (Oka, Katada, Omura, Suwa, Yoshihara, & Touhara, 2006). The ratio of narrowly versus broadly tuned ORs, however, is not known – so far, only ca. 20 % of all human ORs have been assigned activating odorants (Di Pizio, Behr, & Krautwurst, 2020). The biological relevance of broadly tuned ORs remains elusive.

With > 10,000 known volatiles just in foods, the necessity of having broadly tuned receptors among the ca. 400 human ORs appears evident. However, Dunkel et al. (2014) have shown that about 230 aroma-relevant KFOs are necessary and sufficient modular olfactory stimuli to create the aroma-typical chemosensory percepts of most foods (Dunkel et al., 2014). Indeed, our group and others have repeatedly shown that ecological relevant odor categories, such as KFOs and semiochemicals, comprise the best natural agonists for ORs (Dunkel et al., 2014; Haag et al., 2021; Krautwurst & Kotthoff, 2013; Marcinek, Haag, Geithe, & Krautwurst, 2021; NOE, Polster, et al., 2017; Saraiva et al., 2019). Given a considerable overlap between these odor categories (Krautwurst & Kotthoff, 2013), the number of odorants constituting an ecological relevant agonist space may closely match the least number of ca. 300 OR genes actually being expressed in the human olfactory epithelium (Saraiva et al., 2019; Verbeurgt, Wilkin, Tarabichi, Gregoire, Dumont, & Chatelain, 2014), out of about 400 protein-coding human OR genes. Hypothetically, thus, each human OR is at least selective, for one or few odorants from ecological relevant odor categories, for example see (Geithe et al., 2017; Haag et al., 2021; NOE, Polster, et al., 2017). Notably, even more or less broadly tuned ORs may show selectivity towards individual odorants (Geithe, Noe, Kreissl, & Krautwurst, 2017; Kepchia, Sherman, Haddad, Luetje, & Dickens, 2017), or may selectively respond to specific chemical groups of odorants (Ahmed et al., 2018; Jovancevic et al., 2017; Marcinek et al., 2021; Spehr et al., 2003).

Abbreviations: GPCR, G-protein coupled receptor; IL-6, interleukin 6; KFO, key food odorant; MAF, minor allele frequency; NsSNP, non-synonymous single nucleotide polymorphism; OR, odorant receptor; OSN, olfactory sensory neuron; PI, promiscuity index; CDI, chemical diversity index.

* Corresponding author.
E-mail address: d.krautwurst.leibniz-lsb@tum.de (D. Krautwurst).

https://doi.org/10.1016/j.foodchem.2021.131680
Received 18 August 2021; Received in revised form 22 November 2021; Accepted 22 November 2021
Available online 26 November 2021

Broadly tuned ORs, thus, likely play an important role in the molecular perception of complex food aroma and/or semiochemicals ((Geithe et al., 2017; Marcinek et al., 2021), for insects, see: (Bohbot & Dickens, 2012)), by participating, together with other receptors, in odorant-induced receptor activity patterns. Alternatively, they may serve as general odor sensors (Grosmaitre et al., 2009), with an agonist space that overlaps significantly with the entire, however yet unknown, human receptive odorant space.

With regard to their receptive ranges, mouse receptors typically have been examined more thoroughly than human ORs. Per experimental setup, on average, mouse or human ORs were screened with about 140 or 80 odorants, respectively (for numbers and references, see Table S1). Moreover, the compositions of odorant collections used for screening against human ORs in the last decades rarely were biased towards an ecological relevance, but mainly featured synthetic molecules (Trimmer & Mainland, 2017). In general, however, experimental approaches to determine the receptive ranges of individual ORs are sparse. So far, only few studies have put a comprehensive collection of ecological relevant KFOs to the test in screening experiments with single human ORs and their most frequent genetic variants, using the GloSensor™ technology (Geithe et al., 2017; Haag et al., 2021; Marcinek et al., 2021; NOE, Polster, et al., 2017). The identification of $>$ 50 agonists in these studies, thus, emphasized the eminent role of KFOs (Dunkel et al., 2014; Kreissl, Mall, Steinhaus, & Steinhaus, 2019) as OR agonists (Geithe et al., 2017; Haag et al., 2021; Marcinek et al., 2021; NOE, Polster, et al., 2017).

OR2W1 appears to be the most broadly tuned human OR identified, so far. For example, Saito et al. (2009) tested 72 non-KFOs and 21 KFOs against OR2W1, and identified 25 and 12 agonists, respectively (Saito, Chi, Zhuang, Matsunami, & Mainland, 2009). Geithe et al. (2017) tested OR2W1 with 190 KFOs, identified 24 agonists, and demonstrated a considerable overlap in agonist spaces with another broadly tuned receptor OR1A1 (Geithe et al., 2017). In total, 84 agonists, of which the minority (30) were KFOs, have been reported for OR2W1 (Adipietro, Mainland, Matsunami, & Zhang, 2012; Audouze et al., 2014; Chatelain, Veithen, Wilkin, & Philippeau, 2014; Geithe, Noe, Kreissl, & Krautwurst, 2017; Kato, Saito, & Wakisaka, 2016; S. Li et al., 2016; Mainland et al., 2014; Saito et al., 2009; Yu et al., 2015). The odorant collections tested were, however, rarely biased towards ecological relevant volatiles, such as semiochemicals or KFOs, but rather comprised a majority of non-KFOs. When tested together, however, the ratio of validated agonist 'hits' per total number of screened compounds was higher for KFOs than that for non-KFOs, e.g. (Saito et al., 2009). Indeed, KFOs have been suggested to be among the most potent agonists for the majority of human ORs (Dunkel et al., 2014; Geithe et al., 2017; Krautwurst et al., 2013; Marcinek et al., 2021; NOE, Polster, et al., 2017). Moreover, Saraiva et al. (2019) recently demonstrated a correlation between the abundance of human OR-expressing neurons and their function to detect foodborne odorants (Saraiva et al., 2019).

However, the types of assays, their sensitivity, as well as the selection of tested compounds varied largely across all previous studies. Recently, we introduced IL-6-HaloTag®, a new bi-functional *N*-terminal receptor tag, which, together with the GloSensor™ technology (Binkowski, Fan, & Wood, 2009; Geithe, Andersen, Malki, & Krautwurst, 2015), enabled an at least three-fold higher sensitivity with respect to odorant/OR-induced cAMP signaling in test cell systems (NOE, Frey, Fiedler, Geithe, Nowak, & Krautwurst, 2017). We, therefore, hypothesized that our IL-6-HaloTag®/GloSensor™ cAMP-luminescence assay (NOE, Frey, et al., 2017) will reveal an overall KFO-enriched agonist space for OR2W1.

Here, we screened OR2W1 against 187 KFOs, using the IL-6-HaloTag®/GloSensor™ cAMP-luminescence assay in HEK-293 cells. We established EC_{50}-ranked orders of potencies for OR2W1 ref (NCBI reference sequence) and its two most frequent haplotypes, OR2W1 $M_{81}V$ and OR2W1 $D_{296}N$, and analyzed the food-relevant chemical agonist space of OR2W1 using a Maximum Common Substructure search.

2. Materials and methods

2.1. Chemicals

The following chemicals were used: Dulbeccós MEM medium (#F0435), FBS superior (#S0615), L-glutamin (#K0282), penicillin (10 000U/mL)/streptomycin (10 000U/mL) (#A2212), trypsin/EDTA solution (#L2143) (Biochrom, Berlin, Germany), calcium chloride dihydrate (#22322.295), D-glucose (#101174Y), dimethyl sulfoxide (DMSO) (#83673.230), HEPES (#441476L), potassium chloride (#26764.230), and sodium hydroxide (#28244.295) (VWR Chemicals BDH Prolabo, Leuven, Belgium), sodium chloride (#1064041000, Merck, Darmstadt, Germany), D-luciferin (beetle) monosodium salt (#E464X, Promega, Madison, USA).

The key food odorants used were as previously published (Geithe et al., 2017; NOE, Polster, et al., 2017) (see also Table S2), and were sorted according to the ClassyFire classification (see supplemental reference S1). Odor qualities were determined in house (Kreissl et al., 2019).

2.2. Molecular cloning of human OR2W1

The protein-coding region of human OR2W1 (NCBI reference sequence: NM_030903.3) was amplified from human genomic DNA by polymerase chain reaction (PCR), using gene-specific primers (Table S3), ligated with T4-DNA ligase (#M1804, Promega, Madison, USA) *Eco*RI/*Not*I (#R6017/ #R6435, Promega, Madison, USA) into the expression plasmid (#pFN210A SS-HaloTag® CMV-neo Flexi®-Vector, Promega, Madison, USA), and verified by Sanger sequencing (Eurofins Genomics, Ebersberg, Germany) using vector internal primers (Table S4).

2.3. PCR-based site-directed mutagenesis

We generated variants of OR2W1 by two-step PCR-based site-directed mutagenesis as described previously (NOE, Polster, et al., 2017), using gene-specific primers and overlapping mutation primers, carrying the changed nucleotides (Table S5). Final amplicons were then sub-cloned as described above, and verified by Sanger sequencing (Eurofins Genomics, Ebersberg, Germany) using vector internal primers (Table S4).

2.4. Cell culture

We used HEK-293 cells (see supplemental reference S2), a human embryonic kidney cell-line, as a test cell system for the functional expression of recombinant ORs. HEK-293 cells were cultivated as previously described (see supplemental reference S3).

2.5. Luminescence assay

For experiments, cells were plated in a 96-well format (Thermo Scientific™ Nunc™ F96 MicroWell™, white, #137103, Thermo Fisher Scientific Inc., Waltham, USA) with a density of 12,000 cells per well. On the next day, the transfection was performed by using the lipofection method, with each 100 ng/well of the corresponding plasmid-DNA, as well as with 50 ng/well of the receptor transport protein RTP1S (see supplemental reference S4), G protein subunit Gαolf (see supplemental references S5–6), and the pGloSensor™-22F (Binkowski et al., 2009) (Promega, Madison, USA), using ViaFect™ (#E4982, Promega, Madison, USA). The pGloSensor™-22F is a genetically engineered luciferase with a cAMP binding pocket, which allows measuring a direct cAMP-dependent luminescence signal. As a control, we transfected the vector plasmid pFN210A, which lacks the coding information of an OR, together with Gαolf, RTP1S, and cAMP-luciferase pGloSensor™-22F (mock). The amount of transfected plasmid-DNA was equal in OR-

transfected and mock-transfected cells. Lipofectamine® 2000 (#11668027, Thermo Fisher Scientific Inc., Waltham, USA) is a cationic lipid-mediated transfection reagent. The formed nucleic acid – cationic lipid complexes are taken up by the cell through endocytosis and the DNA is translocated to the nucleus for gene expression. We used 0.25 µl Lipofectamine® 2000 per 100 ng plasmid DNA, according to the manufacturer's guidelines, and as described in (NOE, Frey, et al., 2017).

Luminescence assays were performed 42 h post transfection as reported previously (see supplemental reference S3). Tested odorants were according to (Geithe et al., 2017; Haag et al., 2021; NOE, Polster, et al., 2017) (for tested KFOs see Table S2, and for tested non-KFOs Table S6.

2.6. Data analysis of the cAMP luminescence measurements

The raw luminescence data obtained from the Glomax® MULTI + detection system was analyzed using the Instinct Software (Promega, USA). Data points of basal level and data points after odorant application were each averaged. From each luminescence signal, the corresponding basal level was subtracted.

For concentration–response relations, the baseline-corrected dataset was normalized to the maximum amplitude of the reference odorant-receptor pair. The dataset for the mock control was subtracted and EC_{50} values and curves were derived from fitting the function

$$f(x) = \left(\frac{(min - max)}{\left(1 + \left(\frac{x}{EC_{50}}\right)^{Hillslope}\right)} \right) + max$$

to the data by nonlinear regression (SigmaPlot 14.0, Systat Software) (see supplemental reference S7). All data are presented as mean ± SD.

2.7. Analysis of the chemical agonist scaffolds

SMILES format of OR2W1 agonists was used for the ClassyFire chemical taxonomy analysis (see supplemental reference S1). We used a Maximum Common Substructure (MCS) search among analyzed molecules to investigate the chemical similarity of OR2W1 actives and inactives identified in this paper. Specifically, we used heuristic algorithms for the MCS search (see supplemental reference S8), i.e., Library MCS (LibMCS) clustering, as implemented in JChem (see supplemental reference S9).

2.8. Bioinformatics

NCBI was used as database for the retrieval of genetic information on *Homo sapiens* (human) odorant receptor genes (see supplemental reference S10). The phylogenetic reconstruction of ORs was performed with QIAGEN CLC Genomics Workbench 20.0 (https://digitalinsights.qiagen.com/) and MEGA X software (see supplemental reference S11). Therefore, in the first step, all human OR sequences were aligned using ClustalW algorithm (see supplemental reference S12). The evolutionary history was inferred using the Neighbor-Joining method (see supplemental reference S13) followed by 500 bootstrap replications (see supplemental reference S14). Scale bar refers to the evolutionary distances, computed using the Poisson correction method (see supplemental reference S15). Evolutionary analyses were conducted in MEGAX (see supplemental reference S11). For rooting the constructed tree, human rhodopsin (NCBI entry: NP_000530.1) was used as an out-group.

3. Results

Several groups have independently characterized the human receptor OR2W1 as broadly tuned, with to date 84 agonists of which only 30 are KFOs (Adipietro et al., 2012; Audouze et al., 2014; Chatelain et al., 2014; Geithe et al., 2017; Kato et al., 2016; S. Li et al., 2016; Mainland et al., 2014; Saito et al., 2009; Yu et al., 2015). Since KFOs are among the most potent agonists for most human ORs (Dunkel et al., 2014; Geithe et al., 2017; Krautwurst et al., 2013; Marcinek et al., 2021; NOE, Polster, et al., 2017), and since we have shown previously that our IL-6-HaloTag®/GloSensor™ cAMP-luminescence assay (NOE, Frey, et al., 2017) shows higher sensitivity than other previously published assays, we now assumed that we are able to identify an enlarged, KFO-enriched agonist space for OR2W1.

3.1. Screening of OR2W1 versus our chemically diverse KFO library

We tested in total 187 KFOs against OR2W1, each at a concentration of 300 µmol/L (Fig. 1). According to the ClassyFire classification, these compounds are distributed as follows: 2 allyl sulfur compounds, 1 azoline, 14 benzenes and substituted derivatives, 1 benzodioxole, 15 carboxylic acids and derivatives, 2 cinnamic acids and derivatives, 1 cinnamic alcohol, 2 coumarins and derivatives, 6 diazines, 5 dihydrofurans, 25 fatty acyls, 4 heteroaromatic compounds, 1 hydroxy acid, 1 indole, 8 lactones, 2 organic disulfides, 3 organic trisulfides, 48 organooxygen compounds, 2 oxanes, 2 phenol ethers, 16 phenols, 1 phenylpropanoic acid, 17 prenol lipids, 1 pyran, 1 pyridine, 1 pyrroline, 1 thioacetal, 2 thioethers, and 2 thiols (Fig. 1). A Maximum Common Substructures (MCS) clustering analysis revealed 49 chemical clusters for the group of 187 tested KFOs.

3.2. OR2W1 is a broadly tuned odorant receptor with the largest KFO agonist spectrum to date

To validate the hits from our initial KFO-screening, we established concentration–response relations for compounds activating the OR2W1 reference sequence (OR2W1 ref) and its two most frequent haplotypes, OR2W1 $M_{81}V$ (minor allele frequency, MAF: 3.9 %), and OR2W1 $D_{296}N$ (MAF: 24.9 %).

OR2W1 ref responded to 71 of the 187 tested KFOs (Fig. 2, Table 1, Table S7), yielding 0.38 as its promiscuity index (PI) (Di Pizio & Niv, 2015). EC_{50} values < 1000 µmol/L were obtained for the following compounds: 1 allyl sulfur compound (50 % of tested allyl sulfur compounds), 9 benzenes and substituted derivatives (64 %), 1 benzodioxole (100 %), 8 carboxylic acids and derivatives (53 %), 2 cinnamic acids and derivatives (100 %), 1 cinnamic alcohol (100 %), 5 fatty acyls (20 %), 2 heteroaromatic compounds (50 %), 6 lactones (75 %), 1 organic disulfide (100 %), 2 organic trisulfides (67 %), 16 organooxygen compounds (33 %), 1 oxane (50 %), 2 phenol ethers (100 %), 3 phenols (19 %), 10 prenol lipids (59 %), and 1 pyridine (100 %) (Fig. 2, Table 1, Table S7).

Of these, (*Z*)-2-octenal (50), ethyl cinnamate (21), methyl cinnamate (20), cinnamyl acetate (6), 1-octen-3-one (57), 2-phenylethanethiol (2), methyl propyl trisulfide (37), diallyl disulfide (1), (*E*,*Z*)-2,6-nonadienal (54), and 4-isopropylbenzaldehyde (70) resulted to be the ten strongest KFO agonists of OR2W1 (Table 1, Fig. 2, Fig. 3A). Altogether, we identified 48 new KFO agonists of OR2W1 (Table 1).

Some of the compound hits from the screening experiment in Fig. 1 could not be validated, that is they failed to activate OR2W1 in a concentration–dependent manner (data not shown). These inactive KFOs were: hexanal, acetic acid, dimethyl trisulfide, 2,3-diethyl-5-methylpyrazine, 3-mercapto-2-pentanone, (*E*)-2-hexenal, δ-dodecalactone, 2-propionyl-1-pyrroline, 5-ethyl-3-hydroxy-4-methylfuran-2(5*H*)-one (abhexone), 12-methyltridecanal, (*E*)-2-decenal, (*E*)-2-undecenal, and 3-methylphenol, suggesting about 7 % false positives in our screening approach.

Some of the tested substances (Fig. 1, roman numbers, Table S8) showed a concentration-dependent activation of OR2W1 ref, or of one of its haplotypes (OR2W1 $M_{81}V$ or OR2W1 $D_{296}N$), however, only at concentrations or with EC_{50} values above 1000 µmol/L, and therefore have been excluded from the 'actives' set.

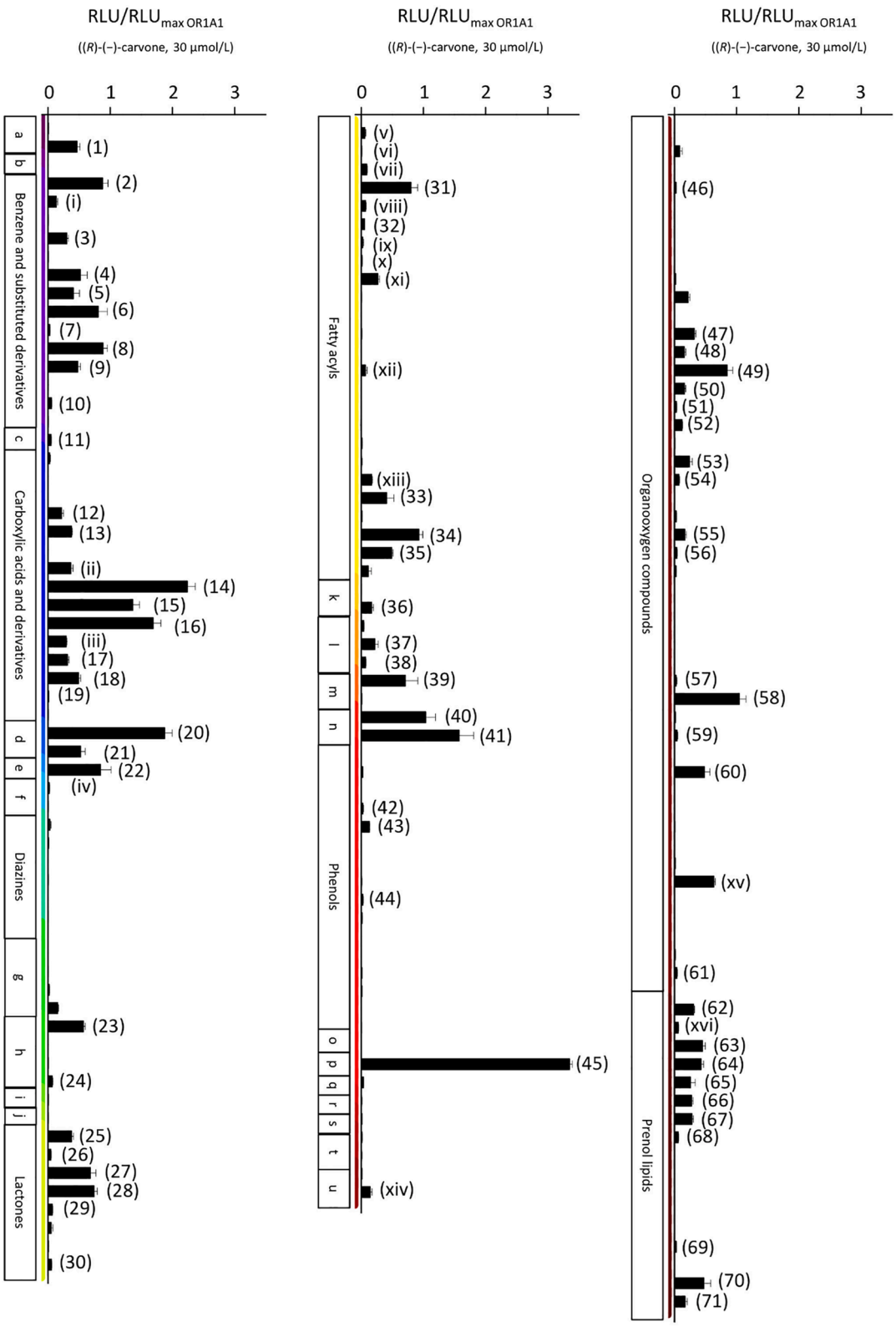

Fig. 1. OR2W1 is activated by 71 Key Food Odorants. Screening of 187 KFOs against the human odorant receptor OR2W1. Shown are mean ± SD (n = 1 measured in duplicates). Mock control was subtracted. Data were normalized to the response of OR1A1 to (*R*)-(−)-carvone (30 µmol/L). The concentration of each KFO was 300 µmol/L. RLU = relative luminescence unit. KFOs are grouped according to the ClassyFire classification. Arabic numbers (see Table 1, Fig. 2) were only shown for those KFOs that could be validated by concentration–response relations with OR2W1. Roman numbers (see Table S8) were only shown for substances that showed concentration-dependent activation but no EC_{50}. a = allyl sulfur compounds, b = azolines, c = benzodioxoles, d = cinnamic acids and derivatives, e = cinnamyl alcohols, f = coumarines and derivatives, g = dihydrofurans, h = heteroaromatic compounds, i = hydroxy acids and derivatives, j = indols and derivatives, k = organic disulfides, l = organic trisulfides, m = oxanes, n = phenol ethers, o = pyrans, p = pyridins and derivatives, q = pyrrolines, r = phenylpropanoic acids, s = thioacetals, t = thioethers, u = thiols.

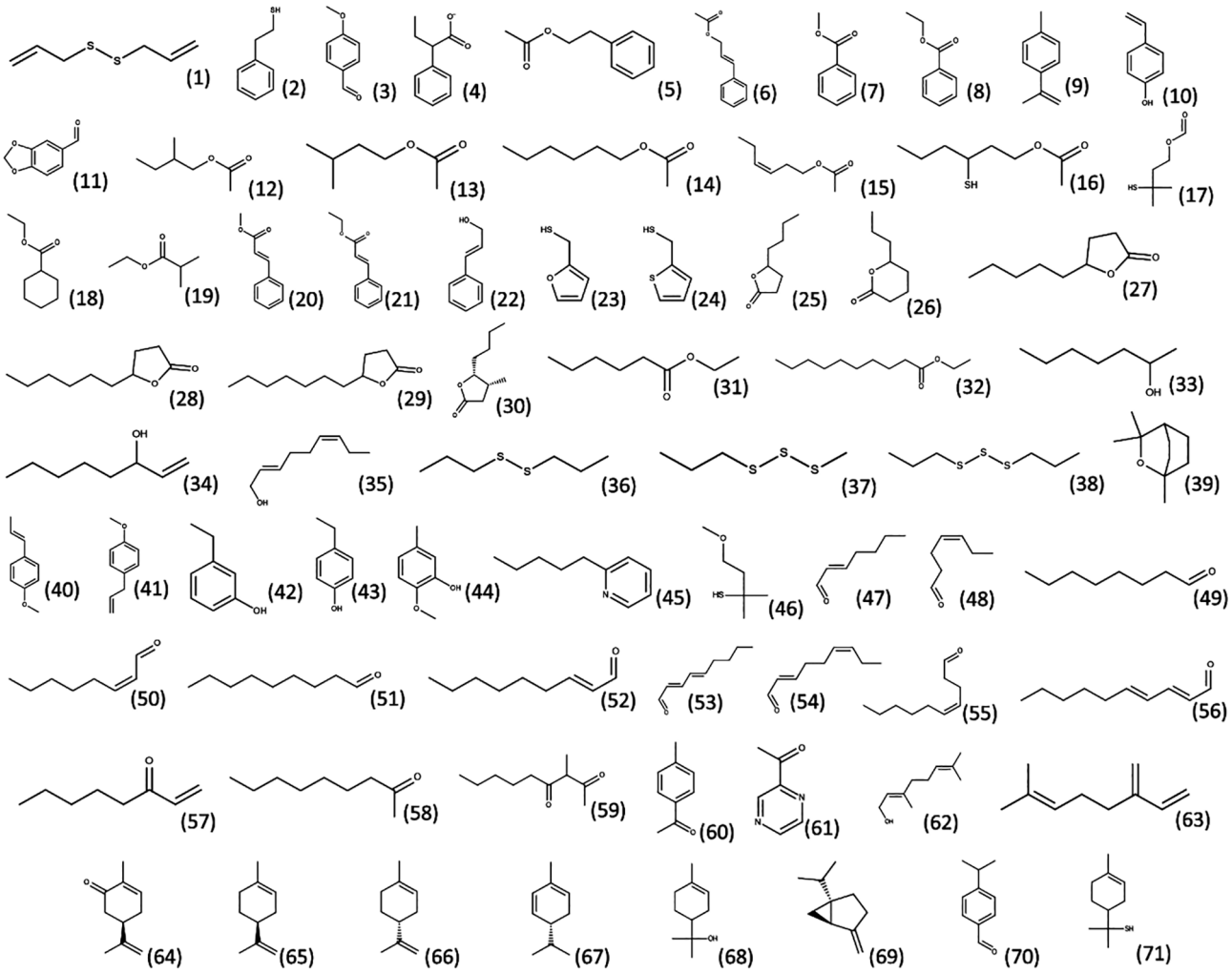

Fig. 2. The KFO agonist spectrum of OR2W1. Structural chemical formulas of the active substances. The numbers result from the affiliation of the individual substance to the respective chemical group according to the ClassyFire classification and their appearance in the KFO screen (Fig. 1, and also refer to Table 1).

We further screened OR2W1 with 14 non-KFOs, structurally related to the KFOs 2-phenylethanethiol, 3-mercaptohexyl acetate, and 2-furfurylthiol, which are among the most potent OR2W1 agonists (Table S6). Specifically, we screened benzyl mercaptan, 1-phenylethyl mercaptan, 2-phenylethanol, 3-phenylpropanol, benzyl methyl sulfide, benzyl methyl disulfide, and benzyl alcohol as structural analogues to 2-phenylethanethiol, and furfuryl alcohol, furfural, 2-methyl-3-furanthiol, furfuryl methyl sulfide, furfuryl methyl disulfide, furfuryl sulfide, and furfuryl disulfide as structural analogues to 2-furfurylthiol. 10 of these 14 compounds activated OR2W1 (Figure S1). Interestingly, furfuryl sulfide, furfuryl disulfide, and benzyl methyl disulfide (Fig. 3B) appeared to be the three best non-KFO agonists for OR2W1, so far (Table 1, Table S9). Concentration-response relationships of the non-KFO compounds on OR2W1 ref and its two haplotypes, OR2W1 $M_{81}V$ and OR2W1 $D_{296}N$, served to validate the screening results (Figure S2, Table S9).

Notably, the six most potent agonists of OR2W1 largely differed in their odor quality, but displayed almost identical EC_{50} values in the low micromolar range. We, therefore, reasoned that to encode odor quality additional receptors must be involved in establishing odorant-selective receptor activation patterns for the majority, if not all OR2W1 agonists identified in our study. As proof of principle, we put a single KFO agonist to the test by vice versa screening it versus 616 variants of our human OR-library. 3-Mercaptohexyl acetate (16), which we had previously assigned functionally to OR2W1 and at least one further receptor, OR1A1 (Geithe et al., 2017; Haag, Ahmed, Reiss, Block, Batista, & Krautwurst, 2019), indeed, activated both receptors, OR2W1 and OR1A1, at a concentration of 100 μmol/L (Figure S3).

3.3. The group of agonists of OR2W1 is chemically diverse and exclusive

In order to visualize the chemotypes covered by the newly identified OR2W1 agonists in this study and by its previously identified agonists, we performed a structure-based clustering of OR2W1 agonists (compounds in Table 1, $EC_{50} < 1000$ μmol/L). We specifically used a MCS approach to identify scaffolds, i.e. the largest substructure, shared by the analyzed compounds. Our analysis revealed 21 clusters of diverse size for all KFO and non-KFO agonists (Fig. 4A), clusters A-U, Table S10, for an enlarged version of Fig. 4A: see supplemental Figure S4, ranging from three singletons (clusters with unique structures) up to two big clusters of 22 and 20 compounds (Fig. 4A, clusters A and D, Table S10 respectively). We identified 13 main scaffolds among KFO agonists. KFO agonists, therefore, are grouped in 13 of the 21 clusters (Fig. 4A, colored clades). Most of the newly discovered OR2W1 agonists could be found in the group of organooxygen compounds (11 agonists) followed by the benzene and substituted derivatives (5 KFO agonists and 5 non-KFO agonists) (Table 1). The first cluster groups molecules that contain an aromatic ring, mostly belonging to the benzenoids/benzene/phenols ClassyFire superclasses, with EC_{50} values ranging from 9.7 to 893.68 μmol/L. The biggest cluster (cluster 4 in Fig. 4A) comprises molecules

Table 1
Comparison of OR2W1 KFO and non-KFO agonists with present literature.

			Present study	Geithe et al., 2017	Li et al., 2016	Kato, Saito, & Wakisaka, 2016	Yu et al., 2015	Audouze et al., 2014	Mainland et al., 2014	Chatelain et al., 2014	Adipietro et al., 2012	Saito et al., 2009
			cell-line									
			HEK-293	HEK-293	Hana3A derived from HEK-293 T stable expression of Gαolf, RTP1L, RTP2, REEP1	HEK-293	Hana3A derived from HEK-293 T stable expression of Gαolf, RTP1L, RTP2, REEP1	Hana3A derived from HEK-293 T stable expression of Gαolf, RTP1L, RTP2, REEP1	Hana3A derived from HEK-293 T stable expression of Gαolf, RTP1L, RTP2, REEP1	HEK-293 T stable expression of RTP1S, RTP2	Hana3A derived from HEK-293 T stable expression of Gαolf, RTP1L, RTP2, REEP1	Hana3A derived from HEK-293 T stable expression of Gαolf, RTP1L, RTP2, REEP1
			co-transfection of Gαolf, Gγ13, RTP1S	co-transfection of Gαolf, Gγ13, RTP1S	co-transfection of RTP1S	co-transfection of RTP1S	co-transfection of RTP1S, M3	co-transfection of RTP1S	co-transfection of RTP1S, M3		co-transfection of RTP1S, M3	co-transfection of RTP1S
			Tag									
			IL-6-HaloTag® assay system	rho-tag(39)	rho-tag(20)	Flag-rho-tag	rho-tag(20)	rho-tag(20)	rho-tag(20)	rho-tag	rho-tag(20)	rho-tag(20)
			GloSensor™ 22F-cAMP Luciferase Assay (Promega)	GloSensor™ 22F-cAMP Luciferase Assay (Promega)	GloSensor™ cAMP Luciferase Assay (Promega)	Dual-Glo™ Luciferase Assay System (Promega)	Dual-Glo™ Luciferase Assay System (Promega)	GloSensor™ 22F-cAMP Luciferase Assay (Promega)	Dual-Glo™ Luciferase Assay System (Promega)	Dual-Glo™ Luciferase Assay System (Promega)	Dual-Glo™ Luciferase Assay System (Promega)	Dual-Glo™ Luciferase Assay System (Promega)
OR2W1 agonists	No.	odor quality (Kreissl et al., 2019)	EC_{50} in μmol/L									
Alkylthiols												
Methanethiol		sulfuric, cabbage-like	not tested		+							
Ethanethiol					+							
Propanethiol					+							
Butanethiol					+							
Pentanethiol					+							
Hexanethiol					+							
Heptanethiol					+							
Octanethiol					+		+				+	*92.68*
Nonanethiol												*86.10*
2-Propanethiol					+							
2-Methyl-1-propanethiol					+							
2-Methyl-2-propanethiol					+							
Allyl sulfur compound												
Diallyl disulfide	(1)	—	17.12 ± 3.04									
Benzene and substituted derivatives												
Cinnamyl acetate	(6)	flowery, rose-like	11.10 ± 0.31	63.74 ± 5.34								
2-Phenylethanethiole	(2)	rubber-like	13.32 ± 0.71	35.16 ± 2.60								
Ethyl benzoate	(8)	starfruit-like	64.46 ± 16.17									
Ethyl 2-phenylacetate	(4)	beeswax-like	75.56 ± 6.04									
p-Anisaldehyde	(3)	woodruff-like, anise-like	235.55 ± 54.82									
Methyl benzoate	(7)	starfruit-like, sweet	260.46 ± 11.91									
2-Phenylethyl acetate	(5)	honey-like, flowery	432.19 ± 68.36	78.72 ± 13.54								
1-Isopropenyl-4-methylbenzene	(9)	terpene-like	756.41 ± 62.30	204.10 ± 9.07								

(*continued on next page*)

Table 1 (*continued*)

			Present study	Geithe et al., 2017	Li et al., 2016	Kato, Saito, & Wakisaka, 2016	Yu et al., 2015	Audouze et al., 2014	Mainland et al., 2014	Chatelain et al., 2014	Adipietro et al., 2012	Saito et al., 2009
4-Vinylphenol	(10)	phenolic, earthy	893.68 ± 275.32									
2-Phenylethanol	(i)	floral, honey-like	> 1000							97.72		
Benzyl methyl disulfide			*7.22 ± 0.23*									
Benzyl methyl sulfide			*41.19 ± 1.52*									
1-Phenylethanethiol			*63.56 ± 3.30*									
Benzyl mercaptan			*81.55 ± 0.80*									
3-Phenylpropanol			*339.29 ± 9.75*									
Benzophenone												*28.84*
1-Phenylbutan-2-one										*6.31*		
3,4-Dimethoxyphenylacetone										*58.88*		
1-Phenylethanol										*158.49*		
Allyl phenylacetate				*43.35 ± 2.50*			+				*0.04*	*15.42*
Benzyl acetate							+	*34.27 ± 1.17*				*16.37*
4-Methoxybenzyl acetate										*1.91*		
Benzodioxoles												
Piperonal	(11)	woodruff-like, vanilla-like	403.86 ± 42.10									
Helional®											+	
Benzoic acid												
Benzyl salicylate							+					
Benzopyran												
4-Chromanone												*90.99*
Carbonyl compound												
Acetophenone												*42.46*
Carboxylic acids and derivatives												
3-Mercaptohexyl acetate	(16)	blackcurrant-like	72.00 ± 6.76	72.04 ± 4.49								
(*Z*)-3-Hexenyl acetate	(15)	green banana-like	105.41 ± 5.70									
Hexyl acetate	(14)	fruity, pear	113.92 ± 10.02	474.45 ± 88.89								13.71
Ethyl cyclohexanecarboxylate	(18)	fruity, sweet	420.28 ± 13.02	365.85 ± 43.18								
3-Mercapto-3-methylbutyl formate	(17)	catty, blackcurrant-like	438.25 ± 25.57									
3-Methylbutyl acetate	(13)	banana-like, fruity	461.66 ± 99.52	615.27 ± 90.18								
Ethyl 2-methylpropanoate	(19)	fruity	539.19 ± 152.96									
2-Methylbutyl acetate	(12)	sweet, fruity	571.55 ± 77.12									
Ethyl 3-(methylthio)propanoate	(iii)	sulfuric, fruity	1522.51 ± 67.28									
Butyl acetate	(ii)	fruity, green	> 1000									
sec-Butyl formate												*37.41*
Prenyl acetate												*84.92*
Cinnamic acids and derivatives												
Ethyl cinnamate	(21)	sweet, cinnamon-like, fruity, soapy	9.70 ± 2.41									

(*continued on next page*)

Table 1 (*continued*)

			Present study	Geithe et al., 2017	Li et al., 2016	Kato, Saito, & Wakisaka, 2016	Yu et al., 2015	Audouze et al., 2014	Mainland et al., 2014	Chatelain et al., 2014	Adipietro et al., 2012	Saito et al., 2009
Methyl cinnamate	(20)	sweet, fruity	10.72 ± 2.02	41.85 ± 2.16								
Cinnamyl alcohols												
Cinnamic alcohol	(22)	flowery	316.41 ± 33.97									
Coumarin												
Coumarin	(iv)	woodruff-like, almond paste-like	> 1000								+	86.10
Fatty acyls												
1-Octen-3-ol	(34)	mushroom-like	57.64 ± 5.12	223.07 ± 13.19								
Ethyl decanoate	(32)	soapy, pear-like	80.07 ± 8.04									
(*E,Z*)-2,6-Nonadienol	(35)	metallic, cucumber-like	106.66 ± 4.88									
Heptan-2-ol	(33)	coconut-like, dill-like	178.30 ± 10.11	433.99 ± 18.45								
Ethyl hexanoate	(31)	fruity, pineapple-like	308.59 ± 30.64									
Ethyl butanoate	(vi)	fruity	2952.30 ± 1744.15									
Octanoic acid	(xii)	carrot-like, musty	> 1000				+					14.22
Ethyl 2-methylbutanoate	(ix)	fruity	> 1000									
Ethyl 3-methylbutanoate	(x)	fruity, blueberry-like	> 1000									
Ethyl octanoate	(viii)	fruity, musty	> 1000									
Methyl butanoate	(v)	fruity	> 1000									
Ethyl pentanoate	(vii)	fruity	> 1000									
Ethyl 4-methylpentanoate	(xi)	fruity	> 1000									
Hexan-1-ol	(xiii)	grassy, marzipan-like	> 1000									14.06
Decanoic acid		soapy, musty	n.d.		+							175.39
Hexanoic acid		sweaty	n.d.			+						
Nonan-1-ol		soapy, fruity	n.d.	89.59 ± 8.59								23.44
(Z)-3-Hexenol		lettuce-like	n.d.						+			
Nonanoic acid					+	+					+	*189.23*
Octan-1-ol							+				+	*7.45*
Heptan-1-ol												*14.76*
Decan-1-ol												*43.15*
Heteroaromatic compounds												
2-Thiophenemethanethiol	(24)	coffee-like, sulfuric	97.77 ± 2.73									
2-Furfurylthiol	(23)	sulfuric, burnt	180.69 ± 18.43									
Furfuryl sulfide			*3.93 ± 0.22*									
Furfuryl disulfide			*4.32 ± 0.16*								+	
Methyl furfuryl disulfide			*11.45 ± 0.54*									
Furfuryl methyl sulfide			*143.00 ± 7.69*									
Furfuryl alcohol			*> 1000*									
Lactones												
γ-Decalactone	(28)	peach-like, coconut-like	78.90 ± 17.54									
γ-Nonalactone	(27)	coconut-like	139.32 ± 14.18									

(*continued on next page*)

Table 1 (*continued*)

			Present study	Geithe et al., 2017	Li et al., 2016	Kato, Saito, & Wakisaka, 2016	Yu et al., 2015	Audouze et al., 2014	Mainland et al., 2014	Chatelain et al., 2014	Adipietro et al., 2012	Saito et al., 2009
γ-Octalactone	(25)	coconut-like	211.81 ± 2.60	483.63 ± 23.15								
γ-Undecalactone	(29)	peach-like	228.23 ± 54.75									
δ-Octalactone	(26)	coconut-like	473.56 ± 229.66									
cis-Whisky lactone	(30)	coconut-like	508.78 ± 25.72									
Organic disulfide												
Dipropyl disulfide	(36)	onion-like	612.76 ± 27.38									
Organic trisulfides												
Methyl propyl trisulfide	(37)	onion-like, roasty, sulfuric	15.86 ± 8.53									
Dipropyl trisulfide	(38)	onion-like, metallic	114.17 ± 10.17									
Organooxygen compounds												
(*Z*)-2-Octenal	(50)	fatty, nutty	8.74 ± 0.12									
1-Octen-3-one	(57)	mushroom-like	12.54 ± 3.90									
(*E*,*Z*)-2,6-Nonadienal	(54)	cucumber-like	19.14 ± 0.43									
(*E*)-2-Nonenal	(52)	fatty, green	32.99 ± 4.03									
(*E*)-2-Heptenal	(47)	green apple-like, bitter almond-like	39.39 ± 9.01	271.02 ± 23.73								
(*E*,*E*)-2,4-Nonadienal	(53)	fatty, green	44.17 ± 8.45									
4-Methylacetophenone	(60)	almond-like, foxy	53.43 ± 8.37	151.28 ± 15.15								
(*Z*)-4-Decenal	(55)	green, musty	75.14 ± 13.12									
(*E*,*E*)-2,4-Decadienal	(56)	fatty, deep-fried	77.39 ± 39.07									
Octanal	(49)	citrus-like, green	108.73 ± 8.95	35.16 ± 1.32			+					43.55
Nonanal	(51)	citrus-like, soapy	124.35 ± 2.30	61.56 ± 4.13							+	252.35
2-Acetylpyrazine	(61)	popcorn-like, roasty	261.92 ± 62.87									
Nonan-2-one	(58)	fruity, musty	359.35 ± 186.24	278.05 ± 23.31								19.91
(*Z*)-4-Heptenal	(48)	fish-like, train-oil-like	432.47 ± 11.09									
3-Methyl-2,4-nonanedione	(59)	hay-like, anise-like, fish-like	482.33 ± 23.00									
4-Methoxy-2-methyl-2-butanethiol	(46)	catty, blackcurrant-like	935.31 ± 188.83									
2-Methyl-1-butanol	(xv)	malty, solvent-like	> 1000									
Hexanal		green, grassy	n.d.									7.91
Heptan-2-one												*7.21*
Octan-3-one												*9.55*
3,4-Hexandione												*16.60*
Heptan-3-one												*33.34*

(*continued on next page*)

Table 1 (*continued*)

			Present study	Geithe et al., 2017	Li et al., 2016	Kato, Saito, & Wakisaka, 2016	Yu et al., 2015	Audouze et al., 2014	Mainland et al., 2014	Chatelain et al., 2014	Adipietro et al., 2012	Saito et al., 2009
Octan-2-one												*39.90*
Dihydrojasmone												*56.75*
Hexan-2-one												*73.28*
Heptanal												*87.90*
2,3-Hexandione												*433.51*
6-Methyl-2,4-heptanedione				*632.26 ± 18.65*								
2,4-Octanedione				*647.63 ± 29.24*								
2,4-Nonanedione				*494.68 ± 20.08*								
1-Cyclohexylethanol										*5.89*		
2-Cyclohexylethanol										*8.32*		
Oxane												
1,8-Cineole	(39)	eucalyptus-like	360.35 ± 33.11									
Phenol esters												
(*E*)-Anethole	(40)	aniseseed-like	92.57 ± 10.63	198.48 ± 7.42								
Estragole	(41)	anise-like, licorice-like	146.97 ± 130.51	162.97 ± 9.83								
4-Allyl-2-methoxyphenyl acetate											+	
Phenols												
4-Ethylphenol	(43)	phenolic	331.23 ± 59.79									
2-Methoxy-5-methylphenol	(44)	smoky, clove-like	513.51 ± 192.61									
3-Ethylphenol	(42)	phenolic, leather-like	513.79 ± 93.80									
1-(4-Hydroxyphenyl)butan-2-one										*15.85*		
Prenol lipids												
4-Isopropylbenzaldehyde	(70)	—	30.96 ± 1.45									
1-*p*-Menthene-8-thiol	(71)	grapefruit-like, sulfuric	81.15 ± 1.59									
(*R*)-(+)-Limonene	(66)	citrus-like	104.10 ± 9.21	111.00 ± 6.76							+	
(*R*)-(-)-Carvone	(64)	mint-like	117.49 ± 8.10	227.25 ± 25.50			+					22.03
(*S*)-(-)-Limonene	(65)	citrus-like	131.62 ± 12.84	100.34 ± 7.86								
Geraniol	(62)	rose-like, citrus-like	159.89 ± 4.79				+					18.37
α-Phellandrene	(67)	terpen-like, dill-like	196.11 ± 10.52									
α-Terpineol	(68)	flowery, citrus-like	354.83 ± 16.96									
(+)-Sabinene	(69)	—	374.46 ± 102.77									
Myrcene	(63)	geranium-like, carrot-like, hop-like	512.44 ± 17.87									
(*R/S*)-Linalool	(xvi)	citrus-like, flowery	> 1000									
(S)-(+)-Carvone											+	*22.59*
(-)-β-Citronellol							+					*7.83*
(+)-Dihydrocarvone												*17.58*

(*continued on next page*)

Table 1 (*continued*)

		Present study		Geithe et al., 2017	Li et al., 2016	Kato, Saito, & Wakisaka, 2016	Yu et al., 2015	Audouze et al., 2014	Mainland et al., 2014	Chatelain et al., 2014	Adipietro et al., 2012	Saito et al., 2009
Citral								*128.70 ± 15.03*				
Citronellal								*270.93 ± 6.40*				
Pyridin												
2-Pentylpyridin	(45)	fatty, tallow-like	61.29 ± 17.12	30.00 ± 6.71								
Thietane												
Thietane					+							
Thiol												
3-Mercapto-1-hexanol	(xiv)	grapefruit-like	> 700									

Compound names represent KFOs, and non-KFOs (*italic*). n.d., no response detected up to 3.0 mmol/L. +, tested as concentration-dependent agonist, but without reported EC_{50} value. –, no odor quality is given.

with aliphatic chains, with EC_{50} values ranging from 8.74 to 508.78 μmol/L. These two big clusters cover more than half of the KFO agonists identified in the present study. The ratio between the number of chemical MCS clusters for all OR2W1 agonists (21 clusters) and the number of clusters of all tested compounds (60 clusters in total) is 0.35, which we may refer to as a chemical diversity index (CDI). The ratio between the number of chemical clusters for all OR2W1 KFO agonists (13 clusters) and the number of clusters of all tested KFOs (49 clusters in total) yielded a CDI of 0.27. Hence, KFO agonists of OR2W1, so far, cover more than one quarter of the chemical space of KFOs, supporting the notion of OR2W1 being a genuine broadly tuned receptor, not only in terms of the sheer number but also in terms of the chemical diversity of associated agonists.

Interestingly, the clustering analysis of OR2W1-inactive molecules resulted in 48 groups (of which 27 are singletons), exemplarily visualized for four groups (Fig. 4B, clusters Ai, Bi, Ji, Ki). Looking at the identified MCSs, we could pinpoint specific chemical moieties that are present only among OR2W1-inactives, and not in the agonist set, for example, pyrazines (Fig. 4B, cluster Bi) and furanones (Fig. 4B, clusters Ji, Ki). Notably, highly selective receptors, that are evolutionary younger than OR2W1 (Fig. 4C), have been reported most recently for alkylpyrazine and furanone KFOs, which did not activate OR2W1 (Haag et al., 2021; Marcinek et al., 2021).

3.4. OR2W1 ref and its variants displayed different ranked orders of potencies for the best 25 agonists

Single amino acid changes based on e.g. non-sysnonymous single nucleotide polymorphisms (nsSNPs) in the gene sequences of ORs or non-chemosensory GPCRs may change their sensitivity or potency-ranked agonist profiles (Geithe & Krautwurst, 2015) (see supplemental references S16–17). We, therefore, established EC_{50}-based ranked orders of potencies for OR2W1 ref and its two haplotypes, OR2W1 $M_{81}V$ and OR2W1 $D_{296}N$ (Fig. 5A). The three most potent KFO agonists ((*Z*)-2-octenal (50), ethyl cinnamate (21) and methyl cinnamate (20)), which had almost identical EC_{50} values on OR2W1 ref (see Table 1), in our hands behaved analogously for all three OR2W1 variants. The overall ranked orders of potencies of OR2W1 $M_{81}V$ and OR2W1 $D_{296}N$, however, deviated from the OR2W1 reference sequence (Fig. 5B). Notably, and in stark contrast to OR2W1 ref, ethyl decanoate (32) and (*E*,*E*)-2,4-decadienal (56) were among the top three agonists of OR2W1 $M_{81}V$, and 2-phenylethanethiol (2) was second best agonist of OR2W1 $D_{296}N$ (Fig. 5B).

4. Discussion

The chemical sense of smell plays an important role in food selection, intake, and acceptance, with the hedonic perception of food (flavor) being the major driver of consumer behavior towards food (see supplemental references S18–19). A hedonic perception of food, however, is largely subjective and depends on many factors, most importantly on the highly individual genotypes of odorant receptor repertoires (see supplemental reference S20). Beyond an identification of food aroma-determining compounds, e.g. KFOs, and a description of their organoleptic properties by analytical food chemistry/molecular sensomics approaches (Dunkel et al., 2014) (see supplemental references S21–22), knowledge on odorant coding at the receptor level (Haag et al., 2021) (see supplemental references S23–24) is crucial for an understanding of individually shaped food hedonics (see supplemental references S25–26).

OR2W1 has been one of the better characterized ORs (Adipietro et al., 2012; Audouze et al., 2014; Chatelain et al., 2014; Geithe et al., 2017; Kato et al., 2016; S. Li et al., 2016; Mainland et al., 2014; Saito et al., 2009; Yu et al., 2015), and has been suggested to be broadly tuned to a chemically diverse agonist space (Chatelain et al., 2014; Geithe et al., 2017; Saito et al., 2009) (see also Table 1).

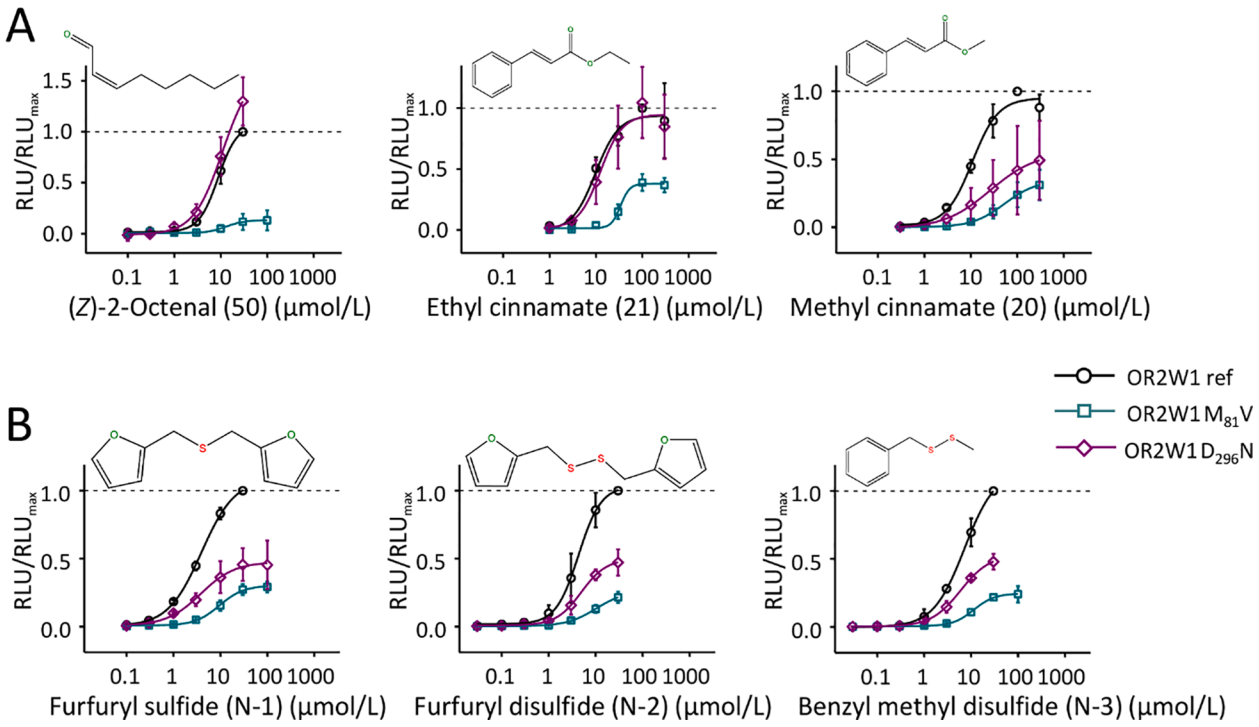

Fig. 3. Concentration-dependencies of most potent KFO and non-KFO agonists of OR2W1 and its variants. Concentration-response relations of (A) the best KFO agonists, (*Z*)-2-octenal (50), ethyl cinnamate (21), and methyl cinnamate (20), and (B) the best non-KFO agonists, furfuryl sulfide (N-1), furfuryl disulfide (N-2), and benzyl methyl sulfide (N-3) on OR2W1 ref and its most frequent haplotypes. Data were mock control-subtracted, normalized to the OR2W1 ref signal of each ligand, and displayed as mean ± SD of independent transfection experiments (n = 3–6). RLU = relative luminescence units. For EC_{50} values, see Table 1.

How many bioassay-validated agonists, and of which chemical diversity, though, of a chemosensory receptor justify its attribute 'broadly tuned'? Displaying a promiscuity index (PI) – which is the number of bioassay-based agonists divided by the total number of tested compounds – of > 0.3, three out of 25 human bitter taste receptors have been identified in the past to be bona fide broadly tuned chemosensory GPCRs, when tested against a chemically diverse library of > 100 bitter compounds (Di Pizio & Niv, 2015) (see supplemental reference S27).

For example, Saito et al. (2009) tested 72 non-KFOs and 21 KFOs against OR2W1, and identified 25 (PI: 0.35) and 12 (PI: 0.57) agonists, respectively (Saito et al., 2009). In the only study, which previously tested a comprehensive set of 190 KFOs, Geithe et al. (2017) identified 18 new KFOs as agonists, and confirmed 6 of its previously reported agonists (PI: 0.13) (Geithe et al., 2017).

Here, by using a sensitivity-improved functional expression system for recombinant ORs (NOE, Frey, et al., 2017), as compared to Geithe et al. (2017), we tested in total 201 odorant compounds, largely represented by 187 KFOs, against OR2W1, and were able to validate 80 agonists via concentration–response relations. From all KFOs tested, we validated 38 % of compounds as agonists of OR2W1 (PI: 0.38), thereby tripling our previously identified KFO promiscuity index of OR2W1 (Geithe et al., 2017).

The results of the present study substantially increased the total number of known OR2W1 agonists that now reaches 153, of which the majority (93 agonists), indeed, are KFOs as defined by Dunkel et al. (Dunkel et al., 2014). Moreover, the identified KFO agonists of OR2W1 represent 27 % (CDI: 0.27) of identified chemical clusters in the group of the 187 KFOs tested in our study, suggesting that OR2W1 has evolved to detect a broad range of chemically diverse KFOs.

We further demonstrate, however, that OR2W1 responded to distinct chemical groups. Surprisingly, and despite being broadly tuned, the KFO agonist profile of OR2W1 specifically excludes e.g. furanones and alkylpyrazines, of which KFOs have been identified most recently as agonists for other, evolutionary younger and rather specialized receptors, OR5K1, OR5M3, and OR8D1 (Adipietro et al., 2012; Haag et al., 2021; Marcinek et al., 2021; Saito et al., 2009). Moreover, even somewhat broadly tuned ORs with a PI < 0.3, nevertheless, often do show selectivity towards individual odors (Geithe et al., 2017), or selectively react to certain chemical groups of odorants (Ahmed et al., 2018; Marcinek et al., 2021; Spehr et al., 2003) (see supplemental reference S28). This suggests an evolutionary recent acquisition of rather selective or even specific ORs. A similar observation has been made for bitter taste receptors. Given their immanent role for avoidance of toxic compounds, Behrens et al. (2014) suggested that smaller functional gene repertoires might be compensated for by a larger molecular receptive range, whereas larger gene repertoires may have allowed the evolution of specialized receptors, selective for compounds with even species-specific relevance (see supplemental reference S29). Ongoing de-orphaning efforts with the large family of human ORs will finally reveal the ratio of broadly versus narrowly tuned receptors.

The two most potent agonists of OR2W1, furfuryl sulfide (N-1) and furfuryl disulfide (N-2), belong to the same cluster of heteroaromatic compounds. These two odorants have not been categorized as KFOs, so far, because of quality criteria, e.g. a lack of quantitation (Dunkel et al., 2014), but nevertheless are indeed food odorants. Both, furfuryl sulfide and furfuryl disulfide, contribute to the aroma of coffee (see supplemental reference S30). Furfuryl disulfide was also found in boiled, refrigerated and reheated chicken (see supplemental reference S31), and contributes to meat flavor (see supplemental reference S32). The next three potency-ranked best agonists, at the same time are the best KFO agonists of OR2W1, which are (*Z*)-2-octenal (50), ethyl cinnamate (21) and methyl cinnamate (20). (*Z*)-2-octenal with its fatty and nutty odor has been found in bread, sour cherry, meat or soybean oil (Kreissl et al., 2019). However, these two cinnamic acids created completely different odor perceptions, with attributes such as sweet, cinnamon-like, fruity, or soapy (Kreissl et al., 2019). Ethyl cinnamate is an important aroma compound in numerous fruits, such as cempedak, passion fruit, and durian, but also in whisky, white wine, or chocolate. In contrast, methyl

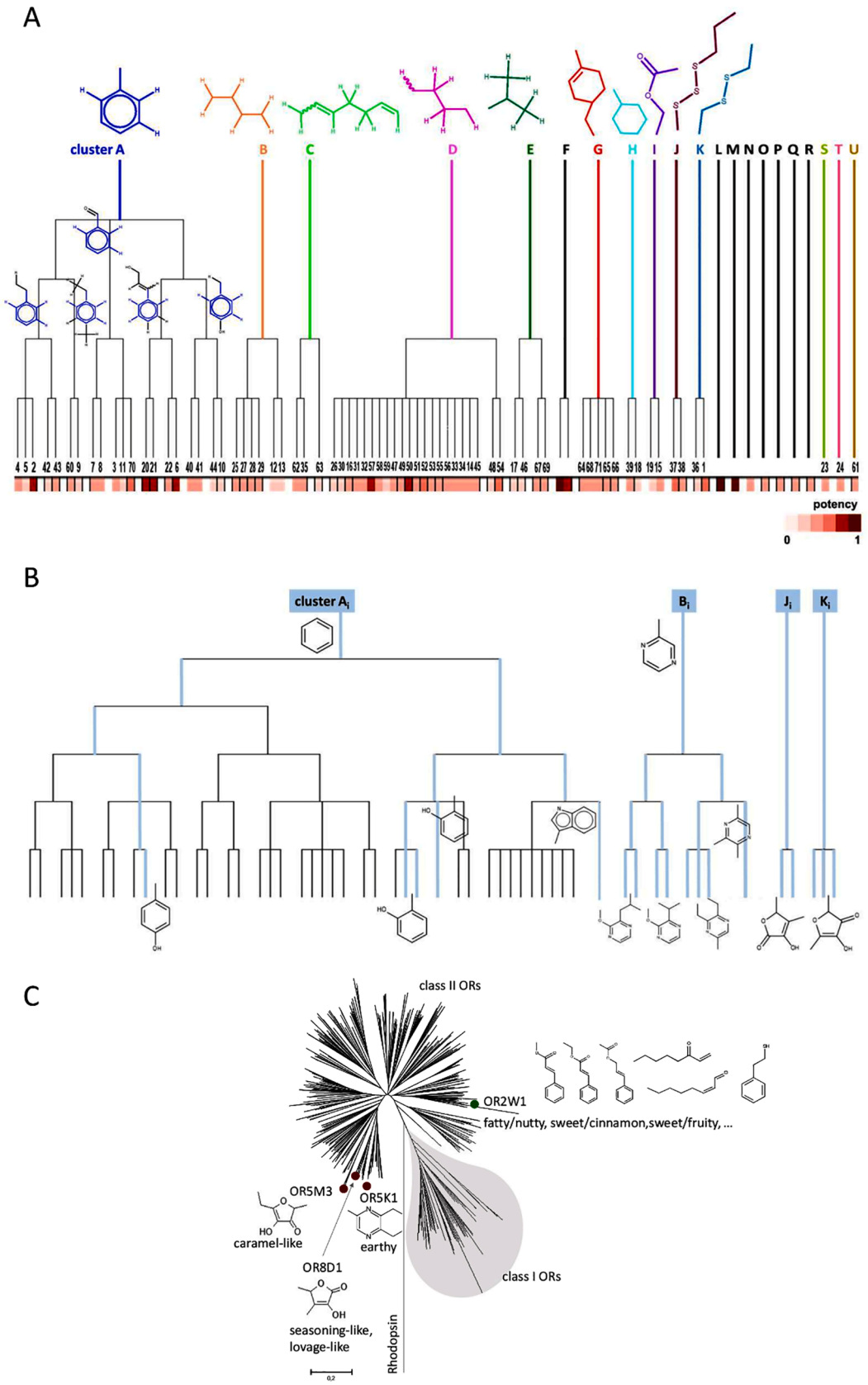

(caption on next page)

Fig. 4. Maximum Common Substructures of OR2W1 agonists are chemically diverse but exclusive. (A) Hierarchical representations of KFO OR2W1 agonists (colored) together with non-KFOs OR2W1 agonists (in black). We report the 2D chemical structures of the MCSs of KFOs and of the nodes of cluster A. Potency (=1/EC_{50}) is normalized to difurfuryl sulfide (non-KFO agonist), which had the lowest EC_{50} value). Letters (A-U) refer to different chemical clusters of agonists (KFOs: colored, Non-KFOs: black). Identified MCSs belong to the classes of benzene and substituted derivatives (A, M, N, O, P, R), heteroaromatic compounds (Q, S, T), hydrocarbons (B, C, D, E, G, H), organic acids and derivatives (J), organoheterocyclic compounds (F, L), organooxygen compounds (U), organosulfur compounds (I, K). Numbers refer to KFO agonist structures given in Table 1, Figs. 1, 2. For an enlarged version of Fig. 4A: see supplemental Figure S4. (B) Hierarchical representations of selected OR2W1 inactives. Highlighted in light blue are the cresol and indole/skatole subclasses (cluster A_i), as well as the pyrazine (cluster B_i), and furanone (clusters J_i, K_i), for which specific receptors are known or can be assumed. (C) Radiale, phylogenetic relationship of all human ORs with human rhodopsin as outgroup. Marked with red dots are phylogenetic younger ORs that are highly selective for their few associated agonists and corresponding odor qualities (Adipietro et al., 2012; Haag et al., 2021; Mainland et al., 2014; Marcinek et al., 2021), which exclusively are not recognized by OR2W1 (green). (For interpretation of the references to colour in this figure legend, the reader is referred to the web version of this article.)

cinnamate has been identified in strawberries, Peruvian ground cherry, and basil, so far (Kreissl et al., 2019).

Altogether, the fact that the so far six best agonists of OR2W1 in the present study had very similar potencies, but represent at least four different odor qualities, ruled out an odor quality-based odorant selectivity of OR2W1, but rather implied that additional receptors must be involved in the detection of these and many other odorants we identified as OR2W1 agonists. Thus, OR2W1 likely participates in odorant-induced activity patterns involving different receptor types, as demonstrated in this study with 3-mercaptohexyl acetate, which proved as an agonist for at least two receptors, OR2W1 and OR1A1, see also (Geithe et al., 2017; Haag et al., 2019). Such combinatorial coding of odorant information at the receptor level likely enables the detection of a multitude of odor qualities exceeding the number of different, single receptor types.

A cautionary note: We may have missed some KFO agonists, because of a lack of sensitivity in our assay. In fact, we excluded odorants with EC_{50} values > 1000 μmol/L. Since we did not screen all known 230 KFOs as reported by (Dunkel et al., 2014), we can not exclude that OR2W1, despite its large and chemically diverse agonist space, may nevertheless display a selectivity towards a yet unknown odorant. We also may have missed further 3-mercaptohexyl acetate (16)-responsive ORs or responsive genetic variants, since our receptor screening experiments did not include all known genetic human OR variants. Moreover, some receptors of our OR library may not work with the assay used in the present study.

While large receptive ranges are unusual for non-chemosensory GPCRs, there are several potential roles for broadly tuned ORs: (i) Odor categories of different origin, relevant for humans, such as food-typical KFOs, off-flavors in food, body odors, semiochemicals, ambient odors, or warning odors against danger and poison, typically are perceived as complex mixtures (Dunkel et al., 2014; Krautwurst et al., 2013; Marcinek et al., 2021) (see supplemental references S33–36). Thus, OR specialists, as well as OR generalists, are needed to implement combinatorial odorant coding at the receptor level (Malnic et al., 1999; Nara et al., 2011) (see supplemental reference S24), enabling an odor quality-specific pattern recognition in the brain, and, thus, the discrimination of single odorants as well as odor bouquets. Several theoretical and data-based models indeed predicted that OR populations that harbor ORs with a broad, partially overlapping range of agonists, or a mixture of narrowly-tuned and broadly-tuned ORs, can enable greater odor coverage (see supplemental references S37–40).

(ii) Another potential role of broadly tuned ORs may be to function as general odor sensors that can cover the largest possible part of the entire odorous substance spectrum. Grosmaitre et al. (2009) characterized the murine receptor Olfr124 (SR1) as a generalist receptor with a particularly broad agonist spectrum, which is expressed in sensory neurons of the septal organ and of the main olfactory epithelium of the mouse (Grosmaitre et al., 2009). The properties of olfactory sensory neurons (OSNs) expressing extremely broadly tuned ORs would make them suited to serve as general odorant detectors and/or sensors for the total odorant concentration (Grosmaitre et al., 2009). However, the transcript levels of OR2W1 in the olfactory epithelium have been reported to be rather low (Saraiva et al., 2019; Verbeurgt et al., 2014). On the other hand, OR2W1 and its mouse homologs have been reported to display rather high basal signaling activities in the absence of agonists (Yu et al., 2015) (see supplemental reference S41), thereby presumably being capable of lowering the threshold of their OSNs for an activation by odorants.

(iii) Alternatively, OR2W1 may function as an extra-nasally expressed chemoreceptor of yet unknown function (see supplemental reference S42).

5. Conclusion

Overall, our work proves successful the testing of a comprehensive collection of chemical ecology-relevant odorants against single receptors, and vice versa, the testing of single compounds against a receptor library, comprising all human ORs, as a functional genomics strategy to characterize the agonist space and/or selectivity of individual ORs.

In summary, we have (i) characterized OR2W1 as the human odorant receptor with, at present, the largest and chemically most diverse, KFO-biased, hence, food-related agonist spectrum, (ii) identified specific chemical moieties that are excluded from this spectrum, but instead are selectively detected by other, evolutionary younger receptors, (iii) demonstrated that naturally occurring, SNP-based changes in amino acid sequence may create receptor variants of different potency-based agonist rankings, and (iv) discussed potential physiological roles of broadly tuned human ORs.

Funding

This research did not receive any specific grant from funding agencies in the public, commercial, ornot-for-profit sectors.

CRediT authorship contribution statement

Franziska Haag: Investigation, Writing – original draft, Visualization. **Antonella Di Pizio:** Formal analysis, Writing – original draft, Visualization. **Dietmar Krautwurst:** Conceptualization, Supervision, Project administration, Writing – review & editing.

Declaration of Competing Interest

The authors declare that they have no known competing financial interests or personal relationships that could have appeared to influence the work reported in this paper.

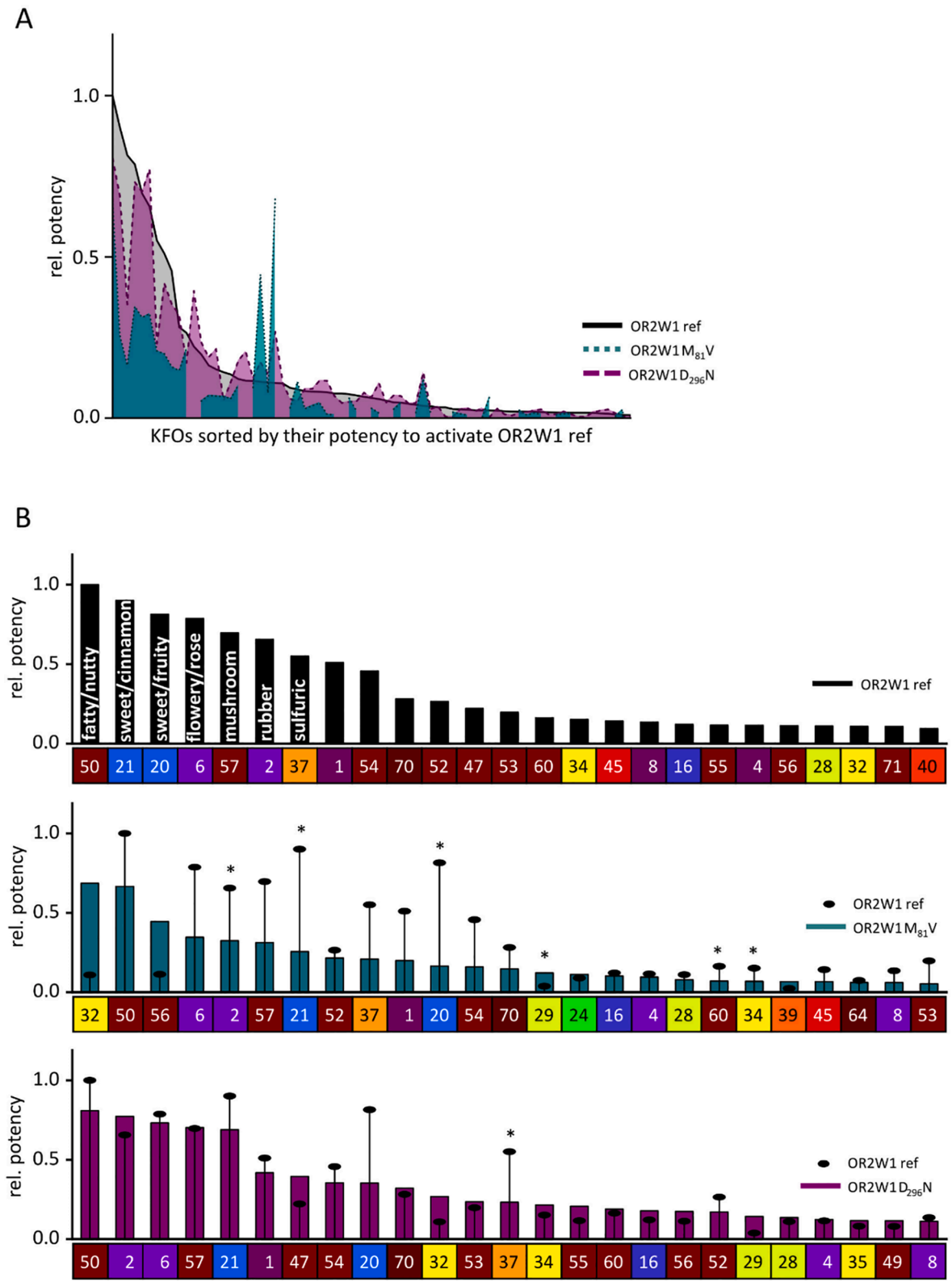

Fig. 5. OR2W1 variants differ in their ranked-order of potencies. (A) Histogram of OR2W1 ref agonists in descending order of their potency (black), as well as of OR2W1 $M_{81}V$ (cyan) and OR2W1 $D_{296}N$ (purple). (B) Ranked orders of potencies for the 25 best agonists of OR2W1 receptor variants. Potencies ($1/EC_{50}$) were always normalized to the potency of compound (50) at OR2W1 ref. For compound names encoded by numbers, and for their mean EC_{50} values and standard deviation, see Tables 1, S7. *, significantly different between OR2W1 ref and respective variant at $p < 0.05$. (For interpretation of the references to colour in this figure legend, the reader is referred to the web version of this article.) (For interpretation of the references to colour in this figure legend, the reader is referred to the web version of this article.)

Acknowledgments

We thank Sandra Hoffmann and Julia Bauer for expert technical assistance, and Maik Behrens for a helpful discussion.

Appendix A. Supplementary data

Supplementary data to this article can be found online at https://doi.org/10.1016/j.foodchem.2021.131680.

References

Adipietro, K. A., Mainland, J. D., Matsunami, H., & Zhang, J. (2012). Functional evolution of mammalian odorant receptors. *PLoS Genetics, 8*(7), e1002821. https://doi.org/10.1371/journal.pgen.1002821

Ahmed, L., Zhang, Y., Block, E., Buehl, M., Corr, M. J., Cormanich, R. A., … Zhuang, H. (2018). Molecular mechanism of activation of human musk receptors OR5AN1 and OR1A1 by (R)-muscone and diverse other musk-smelling compounds. *Proceedings of the National Academy of Sciences of the United States of America, 115*(17), E3950–E3958. https://doi.org/10.1073/pnas.1713026115

Audouze, K., Tromelin, A., Le Bon, A. M., Belloir, C., Petersen, R. K., Kristiansen, K., … Wölfl, S. (2014). Identification of odorant-receptor interactions by global mapping of the human odorome. *PLoS ONE, 9*(4), e93037. https://doi.org/10.1371/journal.pone.0093037

Barwich, A. S. (2016). What is so special about smell? Olfaction as a model system in neurobiology. *Postgraduate Medical Journal, 92*(1083), 27–33. https://doi.org/10.1136/postgradmedj-2015-133249

Baud, O., Etter, S., Spreafico, M., Bordoli, L., Schwede, T., Vogel, H., & Pick, H. (2011). The mouse eugenol odorant receptor: Structural and functional plasticity of a broadly tuned odorant binding pocket. *Biochemistry, 50*(5), 843–853. https://doi.org/10.1021/bi1017396

Binkowski, B., Fan, F., & Wood, K. (2009). Engineered luciferases for molecular sensing in living cells. *Current Opinion in Biotechnology, 20*(1), 14–18. https://doi.org/10.1016/j.copbio.2009.02.013

Bohbot, J. D., & Dickens, J. C. (2012). Selectivity of odorant receptors in insects. *Frontiers in Cellular Neuroscience, 6*, 29. https://doi.org/10.3389/fncel.2012.00029

Chatelain, P., Veithen, A., Wilkin, F., & Philippeau, M. (2014). Deorphanization and characterization of human olfactory receptors in heterologous cells. *Chemistry & Biodiversity, 11*(11), 1764–1781. https://doi.org/10.1002/cbdv.201400083

Di Pizio, A., Behr, J., & Krautwurst, D. (2020). Toward the Digitalization of Olfaction. *Reference Module in Neuroscience and Biobehavioral Psychology*. Elsevier.

Di Pizio, A., & Niv, M. Y. (2015). Promiscuity and selectivity of bitter molecules and their receptors. *Bioorganic & Medicinal Chemistry, 23*(14), 4082–4091. https://doi.org/10.1016/j.bmc.2015.04.025

Dunkel, A., Steinhaus, M., Kotthoff, M., Nowak, B., Krautwurst, D., Schieberle, P., & Hofmann, T. (2014). Nature's chemical signatures in human olfaction: A foodborne perspective for future biotechnology. *Angewandte Chemie (International ed. in English), 53*(28), 7124–7143. https://doi.org/10.1002/anie.201309508

Geithe, C., Andersen, G., Malki, A., & Krautwurst, D. (2015). A butter aroma recombinate activates human class-I odorant receptors. *Journal of Agriculture and Food Chemistry, 63*(43), 9410–9420. https://doi.org/10.1021/acs.jafc.5b01884

Geithe, C., & Krautwurst, D. (2015). Chirality matters and SNPs make the difference - genetic variations on enantiomer-specific odorant receptors for carvone. In A. J. Taylor & D. S. Mottram (Eds.), *Flavour Science: Proceedings of the XIV Weurman Flavour Research Symposium* (pp. 297-302). Leicestershire, U.K.: Context Products Ltd.

Geithe, C., Noe, F., Kreissl, J., & Krautwurst, D. (2017). The broadly tuned odorant receptor OR1A1 is highly selective for 3-methyl-2,4-nonanedione, a key food odorant in aged wines, tea, and other foods. *Chemical Senses, 42*(3), 181–193. https://doi.org/10.1093/chemse/bjw117

Grosmaitre, X., Fuss, S. H., Lee, A. C., Adipietro, K. A., Matsunami, H., Mombaerts, P., & Ma, M. (2009). SR1, a mouse odorant receptor with an unusually broad response profile. *Journal of Neuroscience, 29*(46), 14545–14552. https://doi.org/10.1523/JNEUROSCI.2752-09.2009

Haag, F., Ahmed, L., Reiss, K., Block, E., Batista, V. S., & Krautwurst, D. (2019). Copper-mediated thiol potentiation and mutagenesis-guided modeling suggest a highly conserved copper-binding motif in human OR2M3. *Cellular and Molecular Life Sciences*. https://doi.org/10.1007/s00018-019-03279-y

Haag, F., Hoffmann, S., & Krautwurst, D. (2021). Key Food Furanones Furaneol And Sotolone Specifically Activate Distinct Odorant Receptors. *Journal of Agriculture and Food Chemistry, 69*(37), 10999–11005. https://doi.org/10.1021/acs.jafc.1c03314

Jovancevic, N., Dendorfer, A., Matzkies, M., Kovarova, M., Heckmann, J. C., Osterloh, M., … Hatt, H. (2017). Medium-chain fatty acids modulate myocardial function via a cardiac odorant receptor. *Basic Research in Cardiology, 112*(2). https://doi.org/10.1007/s00395-017-0600-y

Kepchia, D., Sherman, B., Haddad, R., Luetje, C. W., & Dickens, J. C. (2017). Mammalian odorant receptor tuning breadth persists across distinct odorant panels. *PLoS ONE, 12*(9), e0185329. https://doi.org/10.1371/journal.pone.0185329

Krautwurst, D., & Kotthoff, M. (2013). A hit map-based statistical method to predict best ligands for orphan olfactory receptors: Natural key odorants versus "lock picks". *Methods in Molecular Biology, 1003*, 85–97. https://doi.org/10.1007/978-1-62703-377-0_6

Kato, A., Saito, N., & Wakisaka, E. (2016). Method for searching for malodor control agent, malodor control agent, and malodor control method. Patent No. US9233082B2.

Kreissl, J., Mall, V., Steinhaus, P., & Steinhaus, M. (2019). Leibniz-LSB@TUM Odorant Database. Version 1.0. Retrieved from: https://www.leibniz-lsb.de/en/databases/leibniz-lsbtum-odorant-database Accessed.

Li, J., Haddad, R., Chen, S., Santos, V., & Luetje, C. W. (2012). A broadly tuned mouse odorant receptor that detects nitrotoluenes. *Journal of Neurochemistry, 121*(6), 881–890. https://doi.org/10.1111/j.1471-4159.2012.07740.x

Li, S., Ahmed, L., Zhang, R., Pan, Y.i., Matsunami, H., Burger, J. L., … Zhuang, H. (2016). Smelling sulfur: Copper and silver regulate the response of human odorant receptor OR2T11 to low-molecular-weight thiols. *Journal of the American Chemical Society, 138*(40), 13281–13288. https://doi.org/10.1021/jacs.6b06983

Mainland, J. D., Keller, A., Li, Y. R., Zhou, T., Trimmer, C., Snyder, L. L., … Matsunami, H. (2014). The missense of smell: Functional variability in the human odorant receptor repertoire. *Nature Neuroscience, 17*(1), 114–120. https://doi.org/10.1038/nn.3598

Malnic, B., Godfrey, P. A., & Buck, L. B. (2004). The human olfactory receptor gene family. *Proc Natl Acad Sci U S A, 101*(8), 2584–2589. https://doi.org/10.1073/pnas.0307882100

Malnic, B., Hirono, J., Sato, T., & Buck, L. B. (1999). Combinatorial receptor codes for odors. *Cell, 96*(5), 713–723. https://doi.org/10.1016/S0092-8674(00)80581-4

Marcinek, P., Haag, F., Geithe, C., & Krautwurst, D. (2021). An evolutionary conserved olfactory receptor for foodborne and semiochemical alkylpyrazines. *FASEB Journal, 35*(6), Article e21638. https://doi.org/10.1096/fj.202100224R

Nara, K., Saraiva, L. R., Ye, X., & Buck, L. B. (2011). A large-scale analysis of odor coding in the olfactory epithelium. *Journal of Neuroscience, 31*(25), 9179–9191. https://doi.org/10.1523/JNEUROSCI.1282-11.2011

Noe, F., Frey, T., Fiedler, J., Geithe, C., Nowak, B., & Krautwurst, D. (2017). IL-6–HaloTag® enables live-cell plasma membrane staining, flow cytometry, functional expression, and de-orphaning of recombinant odorant receptors. *J Biol Methods, 4*(4), Article e81. https://doi.org/10.14440/jbm.2017.206

Noe, F., Polster, J., Geithe, C., Kotthoff, M., Schieberle, P., & Krautwurst, D. (2017). OR2M3: A highly specific and narrowly tuned human odorant receptor for the sensitive detection of onion key food odorant 3-mercapto-2-methylpentan-1-ol. *Chemical Senses, 42*(3), 195–210. https://doi.org/10.1093/chemse/bjw118

Oka, Y., Katada, S., Omura, M., Suwa, M., Yoshihara, Y., & Touhara, K. (2006). Odorant receptor map in the mouse olfactory bulb: In vivo sensitivity and specificity of receptor-defined glomeruli. *Neuron, 52*(5), 857–869. https://doi.org/10.1016/j.neuron.2006.10.019

Olender, T., Waszak, S. M., Viavant, M., Khen, M., Ben-Asher, E., Reyes, A., … Lancet, D. (2012). Personal receptor repertoires: Olfaction as a model. *BMC Genomics, 13*(1), 414. https://doi.org/10.1186/1471-2164-13-414

Saito, H., Chi, Q., Zhuang, H., Matsunami, H., & Mainland, J. D. (2009). Odor coding by a mammalian receptor repertoire. *Sci Signal, 2*(60), ra9. https://doi.org/10.1126/scisignal.2000016

Saraiva, L. R., Riveros-McKay, F., Mezzavilla, M., Abou-Moussa, E. H., Arayata, C. J., Makhlouf, M., & Logan, D. W. (2019). A transcriptomic atlas of mammalian olfactory mucosae reveals an evolutionary influence on food odor detection in humans. *Sci Adv, 5*(7), eaax0396. https://doi.org/10.1126/sciadv.aax0396

Spehr, M., Gisselmann, G., Poplawski, A., Riffell, J. A., Wetzel, C. H., Zimmer, R. K., & Hatt, H. (2003). Identification of a testicular odorant receptor mediating human sperm chemotaxis. *Science, 299*(5615), 2054–2058. https://doi.org/10.1126/science.1080376

Tazir, B., Khan, M., Mombaerts, P., Grosmaitre, X., & Foxe, J. (2016). The extremely broad odorant response profile of mouse olfactory sensory neurons expressing the odorant receptor MOR256-17 includes trace amine-associated receptor ligands. *European Journal of Neuroscience, 43*(5), 608–617. https://doi.org/10.1111/ejn.2016.43.issue-510.1111/ejn.13153

Trimmer, C., & Mainland, J. D. (2017). Simplifying the Odor Landscape. *Chemical Senses, 42*(3), 177–179. https://doi.org/10.1093/chemse/bjx002

Verbeurgt, C., Wilkin, F., Tarabichi, M., Gregoire, F., Dumont, J. E., Chatelain, P., & Newcomb, R. D. (2014). Profiling of olfactory receptor gene expression in whole human olfactory mucosa. *PLoS ONE, 9*(5), e96333. https://doi.org/10.1371/journal.pone.0096333

Yu, Y., de March, C. A., Ni, M. J., Adipietro, K. A., Golebiowski, J., Matsunami, H., & Ma, M. (2015). Responsiveness of G protein-coupled odorant receptors is partially attributed to the activation mechanism. *Proceedings of the National Academy of Sciences of the United States of America, 112*(48), 14966–14971. https://doi.org/10.1073/pnas.1517510112